

Band Magnetism in A_2T_2Sn ($A = Ce, U; T = Ni, Pd$) from Local Spin Density Functional Calculations

S. F. Matar¹ and A. Mavromaras

ICMCB–CNRS UPR9048, Université Bordeaux I, Avenue du Docteur Albert Schweitzer, F-33608 Pessac Cedex, France

Received October 14, 1999; accepted November 5, 1999

The electronic and magnetic properties of A_2T_2Sn ($A = Ce, U; T = Ni, Pd$) intermetallic systems are self-consistently calculated within the local spin density functional (LSDF) theory using the augmented spherical wave (ASW) method. Trends of the magnetism are discussed in terms of the characteristics of the Ce($4f$) and U($5f$) states as well as the energetic position of the transition metal element d states. © 2000 Academic Press

Key Words: intermetallic cerium and uranium compounds; ASW; LSDA; spin-orbit coupling; orbital moments

INTRODUCTION

The families of ternary intermetallic systems A_2T_2X ($A = Ce, U; T = 3d, 4d$ transition metal; $X = Sn, In$) are well known to exhibit a wide variety of electronic and magnetic properties (1, 2). In these compounds the formation of magnetic moments is governed by the degree of hybridization of the electronic valence states of Ce or U and the respective T and X ligand bands. The physical reasons for the varying hybridization strength can be seen in the bond lengths and in the crystal structure characteristics of these compounds. $4f$ and $5f$ states are known to retain a more or less atomic like character in the solid state. This involves for instance a considerable influence of spin-orbit coupling (SOC) on the narrow f band as well as large orbital effects. In a compound, the mixing of these narrow band states not only depends on their degree of localization but also on the hybridization of the cerium $5d$ and uranium $6d$ states with the T and X ligand valence states. Regarding the uranium-based compounds, the mechanism of intraband spin polarization of the $5f$ states depends on the so-called Hill critical distance, i.e., $d_{U-U} = 3.5 \text{ \AA}$ (3). Generally there is no intraband spin polarization below this value as the U($5f$) band broadens due to the direct overlap of the $5f$ wave functions.

The Ce ($4f$) band is much narrower than the U ($5f$) band. Generally, the localization of the $4f$ states of rare-earth metals and compounds increases with the filling of the $4f$ shell (Lanthanide contraction). Being the first element in the series Ce is considered to be a border case where the degree of localization depends on the applied pressure as well as on the crystal environment. In electronic structure calculations this delicate situation is addressed through various approaches treating the $4f$ states either as atomic like core states or as itinerant in the framework of the local spin density approximation (LSDA) plus possible corrections to the local exchange correlation potential (4). In the framework of the local spin density approximation to the density functional theory we address in this work the effects of hybridization between the respective states of the atomic constituents on the magnetism and on the bonding for U_2Ni_2Sn , U_2Pd_2Sn , Ce_2Ni_2Sn , and Ce_2Pd_2Sn .

CRYSTAL STRUCTURES

The tetragonal structure of U_2Ni_2Sn , U_2Pd_2Sn , and Ce_2Pd_2Sn consists of a stacking along the c axis of two types of prisms (Fig. 1): a square-based one $\{Ce_8\}$ or $\{U_8\}$ around Sn and a trigonal prism $\{Ce_6\}$ or $\{U_6\}$ around the transition element. The structure is derived from an ordered lattice of U_3Si_2 -type with two formula units per cell, i.e., $A_4T_4Sn_2$, where T replaces Si and Ce(U) occupies one of the uranium sites, whereas the other site contains Sn. Every Ce(U) atom is surrounded by seven nearest-neighbor Ce(U). Five of them are situated in the basal plane (a,b), the other two lie along the c axis. The structure can be alternatively described as a succession of planes perpendicular to the c axis with the sequence $(T-Sn)-A-(T,Sn)-A- \dots$ at $z = 0$ and $z = \frac{1}{2}$, respectively. Although of body-centered orthorhombic symmetry with one formula unit per cell, the structure of Ce_2Ni_2Sn shows some resemblance to the U_3Si_2 -type crystal structure with a similar stacking of the sequence $(Ni-Sn)-Ce-(Ni,Sn)$ at $z = 0$ and $z = \frac{1}{2}$, respectively (Fig. 2). The atomic coordinates and the experimental lattice constants were taken from the literature (1, 2).

¹To whom correspondence should be addressed.



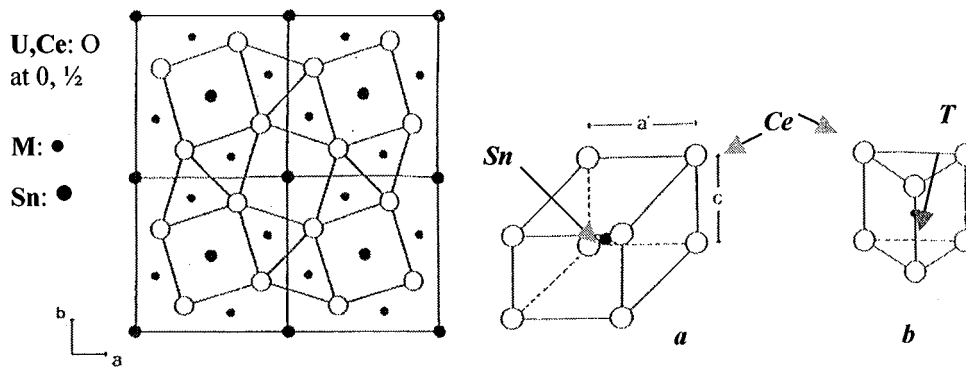


FIG. 1. The U_2Ni_2Sn , U_2Pd_2Sn , and Ce_2Pd_2Sn , systems with projection onto the (001) plane of the structure. The uranium and cerium local environments of Sn (U_8 prism) (a) and T (U_6 prism) (b) are shown.

METHOD OF CALCULATION

All of our investigations (5, 6) are based on *ab initio* electronic structure calculations derived from spin polarized density functional theory (DFT) in its local spin density approximation (LSDA). In particular, we have applied the augmented spherical wave method (ASW) (7) in a scalar relativistic implementation (8) including spin-orbit coupling. For exchange and correlation we used the parametrization scheme of von Barth and Hedin (9) and Janak (10). All valence electrons, including Ce(4*f*)/U(5*f*) were treated as band states. In the minimal ASW basis set (7), we chose the outermost shells to represent the valence states. Energetically low lying Sn(4*d*¹⁰) states which were found to contribute little to the chemical bonding were considered as core states. The matrix elements were constructed using partial waves up to $l_{\max.} + 1 = 4$ for U and Ce and $l_{\max.} + 1 = 3$ for T and Sn. Within the atomic sphere approximation (ASA), the ASW method assumes overlapping spheres centered on the atomic sites where the potential has a spherical symmetry. Our choice of the atomic sphere radii was optimized to reduce the overlap between the spheres. The lattice parameters and atomic positions are the only input to the

calculations. Within the ASA the volume of the spheres is enforced to equal the cell volume so that the remaining interstitial region is neglected from the calculations. A comment on the ASA is in order. The ASA is unproblematic for compact structures such as that of the intermetallic systems. This is because the overlap of the spheres centered on the actual atomic sites can be kept to a minimum (less than 15%) contrary to poorly packed crystal structures where the vacant interstitial sites must be represented by pseudo atoms with $Z = 0$ called *empty spheres* (ES). The introduction of ES is necessary to avoid a too large overlap between the actual atomic spheres. In this context, as opposed to the ASA, the muffin-tin approximation—nonoverlapping spheres—used in the full potential linearized augmented plane waves method (FLAPW (17)) can lead to significantly better results for open structures but should lead to similar results for alloys and intermetallics.

The k space convergence was ensured by using 128 k points in the irreducible wedge of the Brillouin zones. Self consistency was obtained when no variation of the charge transfers ($\Delta Q < 10^{-8}$) and of the total variational energy E_{var} ($\Delta E < 10^{-8}$ Rydberg) was observed upon additional cycles.

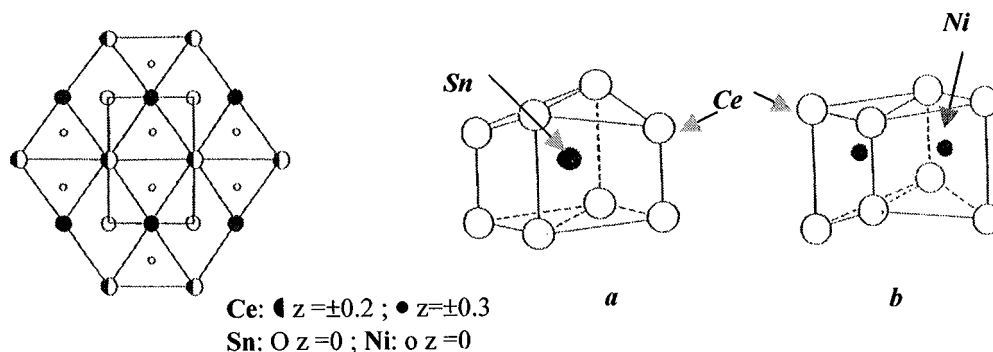


FIG. 2. The Ce_2Ni_2Sn system with projection onto the (001) plane of the structure ($-0.3 \leq z \leq 0.3$). The cerium local environments of (a) Sn (Ce_8 tetragonal distorted prism) and (b) Ni (double Ce_8 trigonal prism).

RESULTS AND DISCUSSION

As a first part of this work, calculations were performed assuming nonmagnetic ground states; i.e., we enforced spin degeneracy for all states. The chemical bonding can be easily addressed from the results of such non-spin polarized (NSP) calculations. This is related to the fact that the spin polarized bands, to a large degree, result from the NSP bands by a rigid band shift. Hence, it is well justified to discuss the mixing between the respective valence states already from the NSP results. Using Stoner theory, the NSP calculations finally allow one to assign a role for each atomic species in the onset of magnetism by intraband spin polarization via the density of states (DOS) at the Fermi level.

Then in a second part, spin only moments were accounted for. Relating to recent works using more sophisticated relativistic calculations for the two uranium intermetallic systems (5, 12), we also investigated the effects of spin-orbit coupling and orbital polarization through an effective orbital field on $\text{Ce}_2\text{Pd}_2\text{Sn}$.

A. Non-Spin-Polarized Calculations

The NSP calculations allow for a simple approach to the bonding in the Ce- and U-based systems from an analysis of the partial site projected DOS from which the hybridization of the electronic states can be determined.

Electronic configurations. Within our choice of the atomic radii little charge transfer could be observed between the different species (e.g., in $\text{U}_2\text{Pd}_2\text{Sn}$ $\Delta Q(\text{U}) = 0.27$ $\Delta Q(\text{Ni}) = -0.33$ $\Delta Q(\text{Sn}) = 0.11$). Testing of other radii expectedly did not change this result significantly. Hence it can be argued for such metallic systems that the bonding mechanism in these systems is mainly driven by the hybridization between the different valence states and not by charge transfer.

Density of states (DOS). The four panels in Fig. 3 show the projected DOS at each lattice site for $\text{U}_2\text{Ni}_2\text{Sn}$, $\text{U}_2\text{Pd}_2\text{Sn}$, $\text{Ce}_2\text{Ni}_2\text{Sn}$, and $\text{Ce}_2\text{Pd}_2\text{Sn}$. The DOS are given for one formula unit, i.e., for 2 (U,Ce), 2 (Ni,Pd), and 1 Sn. The same energy window along the horizontal axis is considered

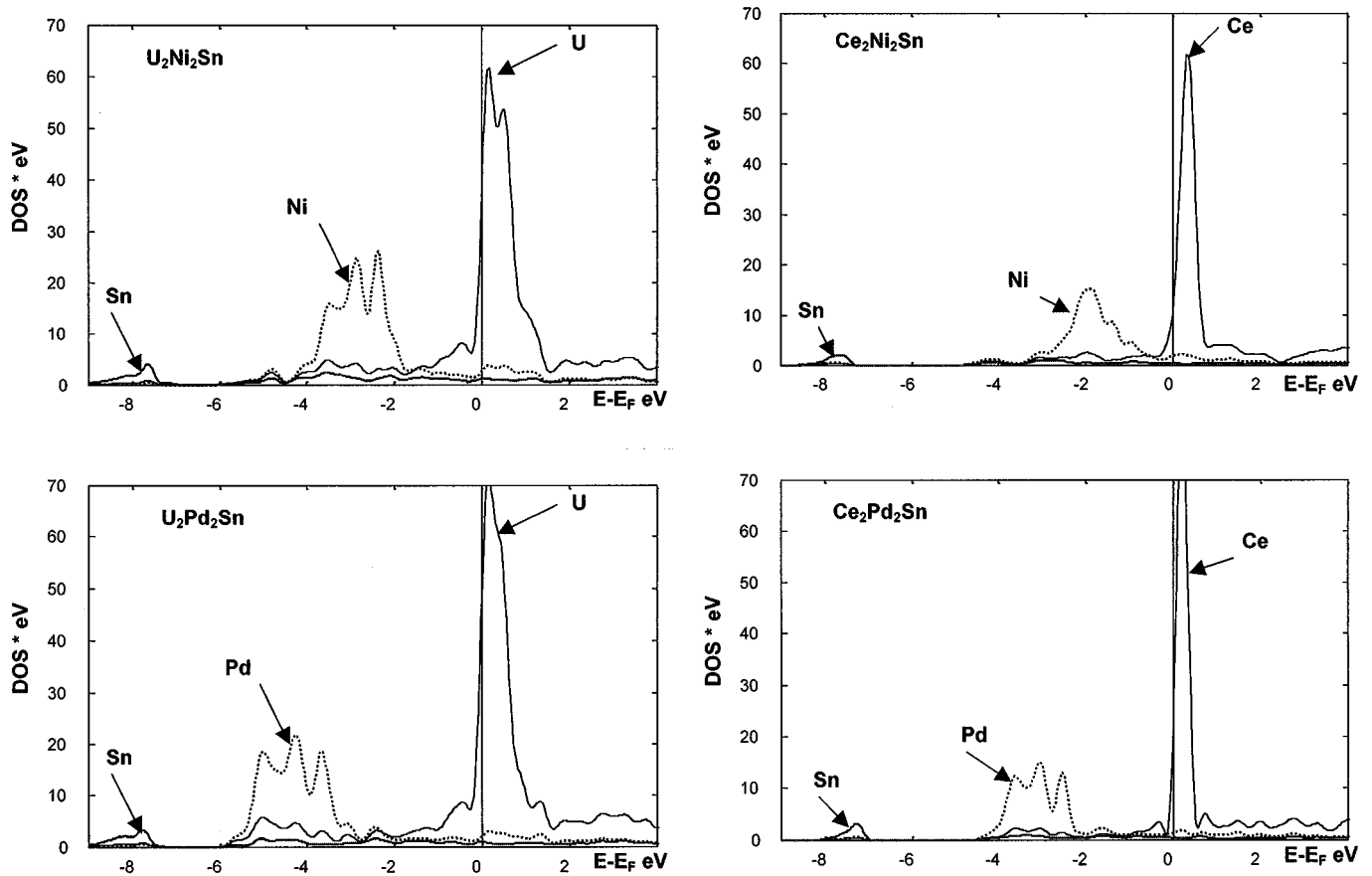


FIG. 3. NSP site projected DOS in $\text{U}_2\text{Ni}_2\text{Sn}$, $\text{U}_2\text{Pd}_2\text{Sn}$, $\text{Ce}_2\text{Ni}_2\text{Sn}$, and $\text{Ce}_2\text{Pd}_2\text{Sn}$.

for all systems and the Fermi level (E_F) is taken as zero energy.

The uranium as well as the cerium DOS show a large peak around E_F mainly due to U($5f$)/Ce($4f$) states, as well as a contribution from itinerant U($6d$)/Ce($5d$) states below E_F which play a larger role in the bonding with the transition metal states. The lower lying energy regions of the U($5f$) and Ce($4f$) DOS are crossed by E_F . The major part of the f bands are unoccupied and thus they are centered above E_F . This is in agreement with the low filling of the uranium and the cerium f subshells with three and two electrons, respectively. As expected, the Ce($4f$) band is narrower than the U($5f$) band, but from Ni- to Pd-based compounds there is a narrowing of the $5f$ and $4f$ peaks (Fig. 3, panels 1 and 2, 3 and 4, respectively). This feature is connected with the weaker hybridization of uranium and cerium states with those of the transition metals. This larger localization should be in favor of a larger moment as it will be shown in sections to follow.

The DOS of Ni and Pd are dominated by the Ni($3d$) and Pd($4d$) states centered around -3 , -4.5 , -2 , and -3.5 eV, respectively. The transition metal $3d$ states are closer to the Fermi level in the case of Ce₂Ni₂Sn compared to their position in the uranium-based compound. An explanation can be found from the different local environment of Ni with the f -metal in the two crystal structures; whereas it is a trigonal prism in U₂Ni₂Sn (Fig. 1) with $d_{U-Ni} = 3.27$ Å, it is a double distorted trigonal prism in Ce₂Ni₂Sn (Fig. 2) with $d_{Ce-Ni} = 3.03$ Å. The difference in the energetical position of the $4d$ states with respect to E_F in the two Pd-based compounds seem to follow the interatomic distances: in U₂Pd₂Sn, d_{Pd-Sn} are shorter than in Ce₂Pd₂Sn (i.e., 2.986 vs 3.057 Å). This leads to a relative energetical downshift of the Pd($4d$) orbitals in the uranium-based compound. As a general trend observed here Ni($3d$) states are energetically closer to E_F than Pd($4d$) (Fig. 3) despite the fact that they belong to the same column so that they can be considered isoelectronic. In the calculations, whether the starting electron configurations of the two transition elements are Ni ($4s^2, 3d^8$) and Pd ($5s^0, 4d^{10}$) or ($5s^2, 4d^8$) a similar occupancy of the d states is obtained at self-convergence for both of them: $n_{Ni(3d)} = 8.78$ electrons in Ce₂Ni₂Sn and $n_{Pd(4d)} = 8.42$ electrons in U₂Pd₂Sn, thus ruling out the aspect of band filling from the origin of the downshift. Further, the energy lowering of Pd($4d$) states vs the top of the filled valence band follows that in the metals themselves: $E_F(\text{Pd}) = 6.8$ eV and $E_F(\text{Ni}) = 9.2$ eV; the difference of 2.4 eV is close to the downshift of the $4d$ band with respect to the $3d$ band in our compounds. From this the stabilization of Pd($4d$) vs Ni($3d$) arises from an atomic effect, whereby $4d$ states are more attracted to the nucleus due to the larger charge of Pd ($Z_{Pd} = 46$; $Z_{Ni} = 28$). In this context we point out to a preliminary calculation of the iso-compositional intermetallic system U₂Pt₂Sn which, although belonging to a different

structure with two uranium sublattices, gives a similar relative energy position of Pt($5d$) to that of Pd($4d$) here. The increased broadness of the d band expected in the series from Ni to Pt is equally observed here.

Consequently, the different bonding between (U, Ce) and T according to whether $T = 3d$ or $4d$ is expected to play a role in the localization of the f states at E_F , thus influencing the magnitude of the nf magnetic moment. Whereas the closeness of Ni($3d$) to the Fermi level favors the mixing with the localized nf states, the position of Pd($4d$) at lower energies leads to a mixing with the broader itinerant d states of uranium and cerium, thus increasing their localization. Finally, it can be pointed out that the difference in shape between the Ni($3d$) DOS in Ce₂Ni₂Sn and the three other intermetallic systems arises from the local crystal environments as shown in Figs. 1 and 2. For instance, we find that the Ni(d_{xz^2})-like orbital in Ce₂Ni₂Sn governs the shape of the Ni DOS, whereas a similar contribution from the d orbitals in the three other isostructural compounds leads to equal contribution from the orbitals to the d DOS.

In all panels of Fig. 3 the dotted lines correspond to the Sn states, which are mainly of p character in the energy range $\{-6, +2\}$ eV. Low lying Sn($5s$) states were observed around -8 eV independently of the compound so that they are not expected to play a major role in the bonding. The relative intensity of the p states from -6 eV up to E_F shows that the mixing between T and Sn is within one plane and occurs at the lower part of T(d) states. A smaller interplane mixing is observed for (U,Ce) and Sn compared to (U,Ce) and T. Thus for the most part the f -element valence states mix with those of the transition metal, preferably through the (d)-like states.

Analysis of the NSP-DOS within Stoner theory. In as far as U and Ce, f and d states were treated as band states in the framework of our calculations, the Stoner theory of band ferromagnetism can be applied to address the spin polarization. Formulating the problem at zero temperature (ground state), one can express the total energy of the spin system resulting from the exchange and kinetic energies counted from a nonmagnetic state as follows: $E = \frac{1}{2}[m^2/n(E_F)] [1 - I \cdot n(E_F)]$. Here I is the Stoner exchange-correlation integral which is an atomic quantity that can be derived from spin-polarized calculations (11) and $n(E_F)$ is the DOS at E_F in the nonmagnetic state. From this expression the product $I \cdot n(E_F)$ provides a criterion for the stability of the spin system. A nonmagnetic configuration (equal occupation of the two spin states) toward spin-polarization (unequal spin occupation) will be unfavorable if $I \cdot n(E_F) > 1$. The system then stabilizes through a gain of energy due to exchange.

In our calculations, the transition metal has a negligible Stoner product throughout and it will not be considered in this analysis. The Stoner products $I \cdot n(E_F)$ for the Ce(U) f/d

states show the following magnitudes: $\text{U}_2\text{Ni}_2\text{Sn}$ (3.43/2.24); $\text{U}_2\text{Pd}_2\text{Sn}$ (5.10/2.80); $\text{Ce}_2\text{Ni}_2\text{Sn}$ (3.08/1.64); $\text{Ce}_2\text{Pd}_2\text{Sn}$ (4.71/2.22). From the larger magnitude of the Stoner product for the f states, the major contribution to the magnetic moment carried by U(Ce) will be expected to arise from the polarization of the $4f$ and $5f$ states and much less contribution will be expected from the d states of U(Ce). Furthermore, these results show that the f moments of the Pd-based systems should be larger than the Ni-based systems.

B. Magnetic (Spin-Polarized SP) Calculations

Next, spin-polarized calculations for the ordered magnetic structures were carried out. This was done by initially allowing for two spin occupations, then self-consistently converging the charges and the magnetic moments. Except for the $\text{U}_2\text{Pd}_2\text{Sn}$ system, which exhibits noncollinear spin configurations (see Ref. (12)), there is no evidence of noncollinear spin arrangements in the other three intermetallic systems so that no use is made here of noncollinear spin calculations. In Table 1 the magnetic moments obtained from spin-only calculations (no spin-orbit coupling) are shown. The trends of the Stoner mean field analysis of the NSP results are confirmed here

- The moment carried by the f element is larger in the Pd-based compounds than in the Ni-based systems.
- The moment carried by the uranium f states is larger than that carried by cerium.
- While we do not explicitly mention them here, the d moments of the f elements are of a low magnitude ($0.1 \mu_B$) for all systems.
- The transition metal carries a vanishingly small moment. Its lowest magnitude is observed for the $\text{Ce}_2\text{Ni}_2\text{Sn}$ system. This probably arises from the small magnetization of Ce itself, whereby the moment on the transition element is probably of an induced nature.

SP-DOS. The effects of spin polarization are illustrated for $\text{Ce}_2\text{Pd}_2\text{Sn}$ in Fig. 4, showing the site projected DOS for Ce and Pd along the two spin directions. Sn states are not shown here for their little contribution to the magnetic moment. In as far as a ferromagnetic order was experimentally found (16), these DOS describe the ground state of

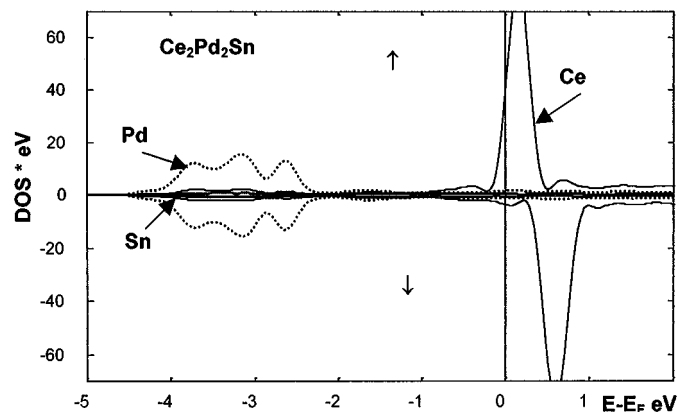


FIG. 4. Spin polarized DOS from spin-only calculations of ordered $\text{Ce}_2\text{Pd}_2\text{Sn}$ in a ferromagnetic configuration.

the system—except for the magnitude of the orbital moment as it will be discussed in next section. The absence of an energetical shift for the Pd DOS points to closely equal spin populations for the majority (\uparrow) and minority (\downarrow) spin populations leading to a vanishingly small magnetic moment carried by the transition metal. Spin polarization does not affect their energy position, which is similar in the NSP DOS (Fig. 3, last panel). On the contrary, there is a relatively large exchange splitting between the (\uparrow) and (\downarrow) bands in the cerium DOS, which illustrates the magnetic moment given in Table 1. The small magnitude of this moment is illustrated by the crossing of the lower part of the $4f$ band with E_F since all of the $f(\downarrow)$ and most of the $f(\uparrow)$ subbands are found above Fermi level.

Spin orbit coupling. It is well known that relativistic effects like spin-orbit coupling (SOC) have considerable influence on the formation of magnetic moments in narrow-band systems such as those based on $4f$ and $5f$ elements. This is of particular importance in the latter, where the size of the SOC splitting is on the order of magnitude of the $5f$ band width. In contrast to $3d$ transition elements, the localized character of the f wave function also leads to the formation of orbital moments. Various attempts have been made in order to include these narrow band correlations into *ab initio* calculational schemes. Here, as in a former work (13) we take into account the correlations leading to Hund's second rule for localized electronic states employing the orbital field (OR) schemes introduced by Brooks (14) and Sandratskii and Kübler (15). In the following, we compare SOC calculations for the ferromagnetic $\text{Ce}_2\text{Pd}_2\text{Sn}$ system with results taken from a work on the uranium analogue $\text{U}_2\text{Pd}_2\text{Sn}$ (12). Table 2 gives the magnetic moments calculated with and without the use of the orbital field correction. Obviously the atomic magnetic moments consist of antiparallel contributions (Hund's rule) from spin and orbital moments where the second is considerably

TABLE 1
Spin Only moments in $\text{U}_2\text{Ni}_2\text{Sn}$, $\text{U}_2\text{Pd}_2\text{Sn}$, $\text{Ce}_2\text{Ni}_2\text{Sn}$
and $\text{Ce}_2\text{Pd}_2\text{Sn}$

Spin only moments	$M(\text{U/Ce}) \mu_B$	$M(T) \mu_B$
$\text{U}_2\text{Ni}_2\text{Sn}$	1.69	-0.05
$\text{U}_2\text{Pd}_2\text{Sn}$	2.20	0.04
$\text{Ce}_2\text{Ni}_2\text{Sn}$	0.68	0.002
$\text{Ce}_2\text{Pd}_2\text{Sn}$	0.85	0.03

TABLE 2
Spin–Orbit Coupling (SOC) and SOC + OR (Orbital Polarization) Results for the Magnetic Moments of Ce₂Pd₂Sn and U₂Pd₂Sn

	$M_S \mu_B$	$M_L \mu_B$	$M_{TOT} \mu_B$	$M_{EXP} \mu_B$	N_f
Ce ₂ Pd ₂ Sn (SOC)	0.78	−0.93	−0.15	1.7–1.86 [16]	1.27
Ce ₂ Pd ₂ Sn (SOC + OR)	1.0	−2.4	−1.4	1.7–1.86	1.35
U ₂ Pd ₂ Sn (SOC) (12)	1.79	−2.7	−0.9	1.9–2.0 [1]	2.95
U ₂ Pd ₂ Sn (SOC + OR) (12)	2.14	−4.07	−1.93	1.9–2.0	3.03

Note. M_s is the spin moment, M_L is the orbital moment, M_{TOT} corresponds to the total magnetic moment, M_{EXP} corresponds to the experimental values, and N_f refers to the electronic occupation of the f bands.

larger than the spin moment. It should be mentioned that the orbital moment of cerium stems from an f occupation of about 1.3 electrons whose orbital moment ($\approx 2.5 \mu_B$) comes close to that of an atomic orbital, namely $3 \mu_B$ as expected from Hund’s second rule. This again reflects the atomic like character of the Ce $4f$ shell. The calculated total moment of $1.5 \mu_B$ (SOC + OR) is found to be in good agreement with the experimentally determined moment (16). Thus the situation is similar to the uranium-based compound as in both cases the introduction of an orbital field yields moments in good agreement with experiment while SOC alone tends to underestimate the orbital and as a consequence the total moment.

CONCLUSION

In this work we have undertaken an investigation of the effects of hybridization of $3d$ and $4d$ transition metal states with localized $4f$ and $5f$ states in four different intermetallic systems. We have shown how the weak d – f hybridization in the two Pd-based compounds leads to stronger localization of the involved f states and hence to larger magnetic moments on the f element site. The different degree of localization of $4f$ and $5f$ states as well as the respective partial

f -band occupations lead to magnetic moments whose magnitudes can only be well accounted for using a full relativistic approach including narrow-band correlations in the form of an orbital field correction term.

ACKNOWLEDGMENTS

Part of the calculations were carried out within the new M3PEC pole of intensive numerical calculations of the University Bordeaux 1. Discussion with Dr. Bernard Chevalier is acknowledged.

REFERENCES

1. A. Purwanto, R. A. Robinson, L. Havela, V. Sechovsky, P. Svoboda, H. Nakotte, K. Prokes, F. R. de Boer, A. Seret, J. M. Winand, J. Rebizant, and J. C. Spirlet, *Phys. Rev. B* **50**, 6792 (1994).
2. F. Mirambet, P. Gravereau, B. Chevalier, L. Trut, and J. Etourneau, *J. Alloys Compounds* **199**, L1 (1993); F. Mirambet, B. Chevalier, L. Fournès, P. Gravereau, and J. Etourneau, *J. Alloys Compounds* **203**, 29 (1993).
3. H.H. Hill, “Plutonium 1970 and Other Actinides” (W. N. Miner, Ed.), Vol. 2. Mat. Soc. Aime, New York, 1970.
4. A. Svane, *Phys. Rev. B* **53** 4275 (1996); P. Söderlind *et al.*, *Phys. Rev. B* **51**(7), (1995).
5. S. F. Matar, *J. Magn. Magn. Mater.* **151**, 263 (1995); S. F. Matar and V. Eyert, *J. Magn. Magn. Mater.* **166**, 321 (1997).
6. S. F. Matar, V. Eyert, S. Najm, B. Chevalier, and J. Etourneau, *J. Mater. Chem.* **8**(5), 1303 (1998).
7. A. R. Williams, J. Kübler, and C. D. Gelatt Jr., *Phys. Rev. B* **19**, 6094 (1979).
8. D. D. Koelling and B. N. Harmon, *J. Phys. C* **10**, 3107 (1977).
9. J. von Barth and D. Hedin, *J. Phys. C* **5**, 1629 (1972).
10. J. F. Janak, *Solid State Commun.* **25**, 53 (1978).
11. J. F. Janak, *Phys. Rev.* **16**, 255 (1977).
12. L. M. Sandratskii and J. Kübler, *Physica B Condens. Matter* **217**, 167 (1996).
13. A. Mavromaras, L. M. Sandratskii, and J. Kübler, *Solid State Commun.* **106**, 115 (1998).
14. M. S. S. Brooks and B. Johansson, “Handbook of Magnetic Materials” (K. H. J. Buschow, Ed.), Vol. 7. Elsevier Science, Amsterdam, 1993.
15. L. M. Sandratskii and J. Kübler, *Phys. Rev. Lett.* **76**, 946 (1995).
16. D. Laffargue, doctorate thesis, University Bordeaux 1, France, 1997.
17. P. Blaha, K. Schwarz, and J. Luitz, “WIEN97,” Vienna University of Technology, 1997. [Improved and updated UNIX version of the original copyrighted WIEN-code, which was published by P. Blaha, K. Schwarz, P. Sorantin, and S. B. Trickey, *Comput. Phys. Commun.* **59**, 399 (1990)]